

Quadrupolar and magnetic ordering in CeB₆

Gennadi Uimin*

Département de Recherche Fondamentale sur la Matière Condensée, SPSMS/MDN, CENG, 17, rue des Martyrs, 38054 Grenoble Cedex 9, France

and Institut für Theoretische Physik, Universität zu Köln, D-50937 Köln, Germany

(Received 24 July 1996; revised manuscript received 28 October 1996)

The quadrupolar ordering in CeB₆ is explained in terms of the electrostatic interaction of quadrupolar moments arranged into a simple cubic lattice. The representation of magnetic and quadrupolar moments by means of quasispins of two kinds is employed. A linear increase of the quadrupolar transition temperature $T_Q(H)$ with applied magnetic field and its further reentrance are described using a generalized spherical model which is well adjusted to a particular problem of the quadrupolar ordering in CeB₆. The theory naturally explains the growing specific heat jump at $T_Q(H)$ with increasing magnetic field. The role of the quadrupolar ordering in the formation of the magnetic ordering, as well as the possible critical experiments and applications to other rare-earth compounds, are discussed. [S0163-1829(97)01013-8]

I. INTRODUCTION

The aim of the present paper is to discuss the nature of the quadrupolar ordering in CeB₆. This compound is classified as a dense Kondo system. With decreasing temperature, the resistivity grows logarithmically, attaining its maximum at $T \approx 3.2$ K.¹ The Kondo temperature was initially estimated as $T_K \approx 8$ K.² Later this value was significantly revised to a value of $T_K \approx 1$ K from the experimental data on the magnetic susceptibility versus temperature.³ This revision was caused by an unusual picture of the crystal field splitting, revealed in the Raman and neutron spectroscopic measurements.⁴

It is well known that the crystalline electric field (CEF) of cubic symmetry (the elementary cell, containing the Ce ion with its boron environment, is shown in Fig. 1) results in splitting of the Ce³⁺ multiplet ($4f^1$, $J=5/2$, $S=1/2$, $L=3$) into a Γ_7 doublet and a Γ_8 quartet. The ground state of Ce³⁺ in CeB₆ is realized as the well isolated Γ_8 quartet, and the Γ_8 - Γ_7 CEF gap has been determined as 47 meV.⁴ Prior to the results of Ref. 4 many difficulties in interpretation of experimental data had arisen in connection with incorrect assumptions on the multiplet splitting: The ground-state level had generally been ascribed to Γ_7 (cf., however, Refs. 5,6). The quadrupolar and magnetic transitions were proved in the specific heat measurements,⁷⁻⁹ NMR,^{10,11} and neutron diffraction^{12,13} studies. Since the typical ordering

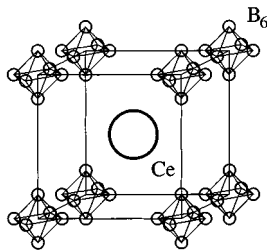


FIG. 1. The elementary cubic cell of CeB₆. Ce ions, as well as boron octahedrals, form simple cubic sublattices with a lattice parameter $a = 4.14$ Å.

temperatures (quadrupolar, $T_Q \approx 3.3$ K, and magnetic, $T_N \approx 2.4$ K) are much smaller than the CEF splitting, for low energy phenomena with T not exceeding several tens K, it should be legitimate to neglect a Γ_7 contribution and to deal with Γ_8 only.

The quadrupolar ordering is characterized by the following features:

(i) There are two lines in the T - H phase diagram, which separate the antiferroquadrupolar (AFQ) phase from the complex antiferromagnetic (AFM) phases (see Fig. 2) and from the disordered (D) phase. The AFQ-D transition line, $T_Q(H)$, exhibits a highly anisotropic behavior. Starting at $T_Q \approx 3.3$ K, T_Q increases with H at not very high magnetic field, and increases linearly, $dT_Q(H)/dH > 0$. The reentrant behavior of $T_Q(H)$, predicted theoretically in Ref. 14, has not yet been confirmed experimentally up to magnetic field of 18 T (Refs. 13,15,16) (for recent experimental data, see Fig. 3). It is worth noting, that the estimates from *below* for the values of the critical field at the reentrance and $T_Q = 0$ are 18 T and 60 T, respectively, according to Ref. 14.

(ii) There are contradictory AFQ patterns obtained in different microscopic measurements: neutron,^{13,15} NMR,¹¹ and μ SR.¹⁷ The interpretation of neutron experiments is consis-

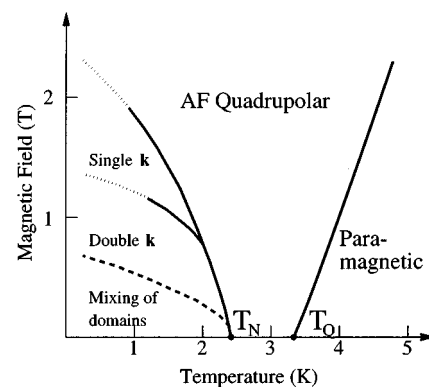


FIG. 2. The low field part of the phase diagram. Positions of the lines, confining the magnetically ordered phases, depend on the orientation of magnetic field.

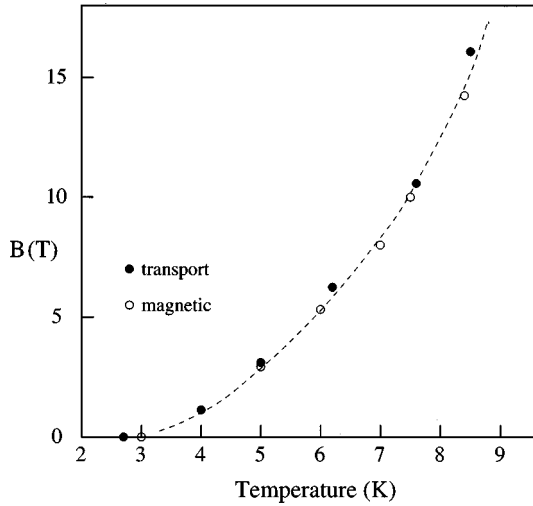


FIG. 3. The boundary between two phases, AFQ and D, as determined experimentally (Ref. 16) by transport (magnetoresistance) and magnetic measurements, full and open circles, respectively. A line is included as a guide to the eye.

tent with the AFQ patterns of the $\mathbf{Q}=[\frac{1}{2}\frac{1}{2}\frac{1}{2}]$ modulation, whereas the NMR and μ SR measurements display more complicated AFQ structures. Note that until now the above-mentioned microscopic methods, i.e., ^{11}B -NMR, neutron diffraction, as well as μ SR, are used in nonzero magnetic fields which generate magnetically ordered states. Indeed, picking up an identical modulation with the AFQ state, a magnetic ordering is a secondary effect with respect to the primary quadrupolar ordering. The theoretical approach developed in Ref. 14 selects the $[\frac{1}{2}\frac{1}{2}\frac{1}{2}]$ structure as energetically preferential.

(iii) The specific heat jump at T_Q appears to be of order of magnitude smaller than its counterpart at $T_N(H=0)$.^{7,9} This points out an important role of fluctuations at the D-AFQ transition. This circumstance has been taken into account in Ref. 14 by employing the spherical model description of the effective spin Hamiltonian. The specific heat jump on the D-AFQ transition line grows with H .⁹

The main features of the magnetic ordering have been presented in Ref. 13:

(i) With a magnetic field applied along $[111]$, the AFM-structure is characterized by the wave vector, either $\mathbf{k}_1=[\frac{1}{4}\frac{1}{4}\frac{1}{2}]$ or $\mathbf{k}_2=[\frac{1}{4}\frac{1}{4}\frac{1}{2}]$ (the single- \mathbf{k} structure at sufficiently high magnetic field), by a couple of \mathbf{k} 's, \mathbf{k}_1 and \mathbf{k}_2 (the double- \mathbf{k} structure in moderate fields), and by a mixture of differently oriented domains at weak magnetic fields (see Fig. 2, where all these magnetic phases are sketched out).

(ii) The Bragg peaks at the wave vectors \mathbf{k}_1 and/or \mathbf{k}_2 are accompanied by $\mathbf{k}_1=[\frac{1}{4}\frac{1}{4}0]$ and/or $\mathbf{k}_2=[\frac{1}{4}\frac{1}{4}0]$, respectively.¹³ Their occurrence is a sign of a crucial role of the AFQ modulation, $\mathbf{Q}=[\frac{1}{2}\frac{1}{2}\frac{1}{2}]$, in the formation of magnetic structures. A possible double- \mathbf{k} structure, identified in Ref. 13, is shown in Fig. 4.

In the next section an effective ‘‘separation’’ of spin and orbital degrees of freedom is carried out by introducing a formalism, according to which magnetic and quadrupolar moments can be properly described by means of two Pauli matrices, $\boldsymbol{\sigma}$ and $\boldsymbol{\tau}$. Section III concerns the analysis of the

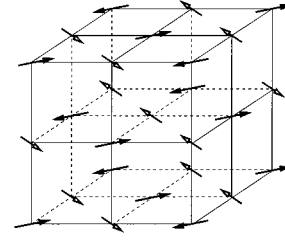


FIG. 4. One of the possible arrangements of magnetic moments in the double- \mathbf{k} structure.

AFQ ground state and relevant excitations. In Sec. IV, on the basis of the two relevant interactions, Zeeman and quadrupolar, and using the spherical model for picking up these interactions, we are able to determine the shape of $T_Q(H)$. It occurs to be strongly anisotropic in the T - H plane. Despite a perfect cubic lattice symmetry, such a strong anisotropy is due to a spacial anisotropy of the quadrupolar interaction. Its conventional form, following from the Coulomb's interaction, gives rise to a very soft mode of τ excitations in the particular case of a simple cubic lattice. Experimentally, strong fluctuations are indicated by a small specific heat jump at the D-AFQ transition. This is a reason for employing the spherical model which is an appropriate tool for describing systems with developed fluctuations.

The spherical model is applied for deriving analytical formulas for the specific heat near the AFQ-D transition. We also outline how the magnetically ordered state can be generated by the quadrupolar interaction via quantum fluctuations of orbital-like ‘‘spins,’’ τ 's. In Sec. V the σ - τ representation is used for the case of a single f hole (configuration f^{13}), which is likely ascribed to the rare-earth compound TmTe. In the concluding section we discuss what kind of experiments could be critical for establishing the nature of the AFQ order unambiguously.

II. THEORETICAL PREREQUISITE

A. Representation of moments through the Pauli matrices. Zeeman interaction

We represent the set of the Γ_8 states with use of the $|\mathcal{J}_z\rangle$ (abbreviation for $|L, S, \mathcal{J}, \mathcal{J}_z\rangle$) basis in the following form:

$$\psi_{1,\pm} = \sqrt{5/6}|\pm 5/2\rangle + \sqrt{1/6}|\mp 3/2\rangle, \quad \psi_{2,\pm} = |\pm 1/2\rangle. \quad (1)$$

The quartet constituents in Eq. (1) are labeled in such a way in order to make use of the Pauli matrices, $\boldsymbol{\sigma}$ and $\boldsymbol{\tau}$, convenient. For each ℓ , the Kramers doublet $\psi_{\ell,\pm}$ is defined as

$$\sigma_z \psi_{\ell,\pm} = \pm \frac{1}{2} \psi_{\ell,\pm}, \quad \sigma_+ \psi_{\ell,-} = \psi_{\ell,+} (\sigma_- \psi_{\ell,+} = \psi_{\ell,-}). \quad (2)$$

The orbital doublet $\psi_{1,\sigma}$ and $\psi_{2,\sigma}$ can be suitably defined with using the pseudospin operator $\boldsymbol{\tau}$ as

$$\begin{aligned}\tau_z \psi_{1,\sigma} &= \frac{1}{2} \psi_{1,\sigma}, & \tau_z \psi_{2,\sigma} &= -\frac{1}{2} \psi_{2,\sigma}, \\ \tau_+ \psi_{2,\sigma} &= \psi_{1,\sigma} & (\tau_- \psi_{1,\sigma} &= \psi_{2,\sigma}).\end{aligned}\quad (3)$$

This representation was proposed in Ref. 6; however, expressions for the magnetic moment in terms of $\boldsymbol{\sigma}$ and $\boldsymbol{\tau}$, given in Ref. 6, are oversimplified.

In order to derive formulas for the moments (\mathbf{J} , \mathbf{S} , \mathbf{L} , \mathbf{M}), we need to calculate the matrix elements of, say, \mathbf{J} over the set $\{\psi_{\ell,\sigma}\}$:

$$\begin{aligned}\langle \psi_{1,\pm} | \mathcal{J}_z | \psi_{1,\pm} \rangle &= \pm 11/6, & \langle \psi_{2,\pm} | \mathcal{J}_z | \psi_{2,\pm} \rangle &= \pm 1/2, \\ \langle \psi_{2,\mp} | \mathcal{J}_z | \psi_{1,\pm} \rangle &= 2/\sqrt{3}, & \langle \psi_{1,\mp} | \mathcal{J}_z | \psi_{2,\pm} \rangle &= 2/\sqrt{3}, \\ \langle \psi_{1,\pm} | \mathcal{J}_x | \psi_{1,\mp} \rangle &= 5/3, & \langle \psi_{2,\pm} | \mathcal{J}_x | \psi_{2,\mp} \rangle &= 3.\end{aligned}\quad (4)$$

Within the Russell-Saunders scheme, the matrix elements of the moments can be obtained from their \mathcal{J} counterpart in accordance with g factors of the f^1 multiplet:

$$\begin{aligned}\langle \cdots S \cdots \rangle &= -\frac{1}{7} \langle \cdots \mathcal{J} \cdots \rangle, & \langle \cdots L \cdots \rangle &= \frac{8}{7} \langle \cdots \mathcal{J} \cdots \rangle, \\ \langle \cdots M \cdots \rangle &= \frac{6}{7} \mu_B \langle \cdots \mathcal{J} \cdots \rangle.\end{aligned}$$

Using the matrix elements (4) we can express the operator of magnetic moment \mathbf{M} , which is associated with Γ_8 as follows:

$$M_i = 2\mu_B \sigma_i \left(1 + \frac{8}{7} T_i \right), \quad i = x, y, z, \quad (5)$$

where

$$T_z = \tau_z, \quad T_x = -\frac{1}{2} \tau_z + \frac{\sqrt{3}}{2} \tau_x, \quad T_y = -\frac{1}{2} \tau_z - \frac{\sqrt{3}}{2} \tau_x. \quad (6)$$

The derivation of formulas (5) from the set of matrix elements (4) is outlined in Appendix A. Note that the τ_y component is not involved in Eq. (5). For the Zeeman interaction

$$\mathcal{H}_Z = -H_i \sum_{\mathbf{r}} M_i(\mathbf{r}), \quad (7)$$

we shall use representations (5) and (6). In Eq. (7) the sum runs over the Ce lattice sites. As usual, summation over repeated indices (i , Cartesian coordinates) is supposed.

Let us discuss some simple properties of Hamiltonian (7), which are important in experimental applications to CeB₆.

(1) If the ‘‘orbital,’’ i.e., τ subsystem exhibits some AFQ order characterized by the modulation vector \mathbf{Q} , then at $H \neq 0$ the effective Zeeman term, acting on σ 's, produces, *first*, the uniform σ component, and *second*, the \mathbf{Q} -modulated σ components. Both are absent in zero field. As a result, a *uniform* magnetic field causes the \mathbf{Q} -modulated magnetization. This property of the AFQ phase has been used in neutron, NMR, and μ SR experiments. In the weak-field region, with H not exceeding few T, the \mathbf{Q} -modulated magnetization is linear in H .

(2) In the magnetically ordered phase (see Fig. 2) the Bragg peaks are related either to the single \mathbf{k} structure (either $\mathbf{k}_1 = [\frac{1}{4}\frac{1}{4}\frac{1}{2}]$, or $\mathbf{k}_2 = [\frac{1}{4}\frac{1}{4}\frac{1}{2}]$), or to the double \mathbf{k} structure (\mathbf{k}_1 and \mathbf{k}_2). These peaks at \mathbf{k}_1 and \mathbf{k}_2 are accompanied by the Bragg peaks at $\mathbf{k}_1 = [\frac{1}{4}\frac{1}{4}0]$ and $\mathbf{k}_2 = [\frac{1}{4}\frac{1}{4}0]$. This fact can be easily understood if we note that magnetization (5) is related not only to the σ modulations (wave vectors \mathbf{k}_1 and/or \mathbf{k}_2), but also to the $(\sigma \cdot \tau)$ modulations. The latter correspond to wave vectors $\mathbf{k}_1 + \mathbf{Q}$ and/or $\mathbf{k}_2 + \mathbf{Q}$ with $\mathbf{Q} = [\frac{1}{2}\frac{1}{2}\frac{1}{2}]$.

(3) Noninteracting Γ_8 ionic states can be realized practically, say, in La_{1-x}Ce_xB₆. Owing to a nontrivial form of the Zeeman interaction, magnetization is not aligned with \mathbf{H} except for a few special H orientations, e.g., [001], [110], [111], and their equivalents. At fixed H the bigger energy gain is achieved for directions of the [001] type. This kind of \mathbf{H} anisotropy is an inherent property of the well-isolated Γ_8 states.

B. Quadrupolar interaction

Not only the vector moments, but the quadrupolar moment Q_{ij} ($i, j = x, y, z$) on a Ce site as well, can be expressed in terms of the $\boldsymbol{\sigma}$ and $\boldsymbol{\tau}$ operators. For calculating the matrix elements of Q_{ij} over the set $\{\psi_{\ell,\sigma}\}$,

$$\begin{aligned}\langle \psi_{\ell,\sigma} | Q_{ij} | \psi_{\ell',\sigma'} \rangle \\ = e \int d^3 r \psi_{\ell,\sigma}^*(\mathbf{r}) \psi_{\ell',\sigma'}(\mathbf{r}) (3x_i x_j - \delta_{ij} r^2),\end{aligned}$$

we can employ the Wigner-Eckhart theorem, according to which these matrix elements are proportional to the operator equivalents:

$$\langle \cdots | Q_{ij} | \cdots \rangle \propto \left\langle \cdots \left| \frac{1}{2} (\mathcal{J}_i \mathcal{J}_j + \mathcal{J}_j \mathcal{J}_i) - \frac{1}{3} \delta_{ij} \mathbf{J}^2 \right| \cdots \right\rangle.$$

Given below are the matrix elements of the quadrupolar moment; we measure them in units of

$$Q_0 = \langle \psi_{1,\sigma} | Q_{zz} | \psi_{1,\sigma} \rangle,$$

i.e.,

$$Q_0 = e \int d^3 r \psi_{1,\sigma}^*(\mathbf{r}) \psi_{1,\sigma}(\mathbf{r}) (3z^2 - r^2). \quad (8)$$

The Q matrix elements can be classified as σ independent

$$\begin{aligned}\langle \psi_{1,\sigma} | Q_{zz} | \psi_{1,\sigma} \rangle &= -\langle \psi_{2,\sigma} | Q_{zz} | \psi_{2,\sigma} \rangle = 1, \\ \langle \psi_{1,\sigma} | Q_{xx} | \psi_{1,\sigma} \rangle &= \langle \psi_{1,\sigma} | Q_{yy} | \psi_{1,\sigma} \rangle = -1/2, \\ \langle \psi_{2,\sigma} | Q_{xx} | \psi_{2,\sigma} \rangle &= \langle \psi_{2,\sigma} | Q_{yy} | \psi_{2,\sigma} \rangle = 1/2, \\ \langle \psi_{2,\sigma} | Q_{xx} | \psi_{1,\sigma} \rangle &= -\langle \psi_{1,\sigma} | Q_{yy} | \psi_{2,\sigma} \rangle = (\sqrt{3}/2),\end{aligned}\quad (9)$$

as well as the σ dependent

$$\begin{aligned}\langle \psi_{2,+} | Q_{xy} | \psi_{1,+} \rangle &= \langle \psi_{1,-} | Q_{xy} | \psi_{2,-} \rangle = i(\sqrt{3}/8), \\ \langle \psi_{2,-} | Q_{yz} | \psi_{1,+} \rangle &= \langle \psi_{2,+} | Q_{yz} | \psi_{1,-} \rangle = i(\sqrt{3}/8), \\ \langle \psi_{2,+} | Q_{zx} | \psi_{1,-} \rangle &= -\langle \psi_{1,+} | Q_{zx} | \psi_{2,-} \rangle = (\sqrt{3}/8).\end{aligned}\quad (10)$$

We omit the Hermitian conjugated matrix elements in Eqs. (9) and (10).

The matrix $\|Q\|$ can be written in the operator form as (see Appendix A for elementary explanations)

$$\|Q\| = Q_0 \begin{pmatrix} 2T_x & \mu_z & \mu_y \\ \mu_z & 2T_y & \mu_x \\ \mu_y & \mu_x & 2T_z \end{pmatrix}, \quad (11)$$

where $\mu_i = (\sqrt{3}/2)\tau_y\sigma_i$. The fact that Q_{ij} contains the σ variables signals that the quadrupolar interaction can be responsible not only for pure orbital interactions, but also for magnetic interactions.

The dependences of M_i and Q_{ij} on σ and τ determine the time-reversal properties of the σ and τ components. It is evident from Eq. (5) that $\sigma \rightarrow -\sigma$ under $t \rightarrow -t$, whereas τ_x and τ_z are unchanged. The off-diagonal components of Q_{ij} require $\tau_y \rightarrow -\tau_y$ under the time-reversal transformation.

We suppose that the predominant contribution to the interactions of Ce ions in CeB₆ comes from their quadrupolar interaction, the role of which in Ce compounds was first mentioned by Bleaney¹⁸ (for a discussion on various forms of the quadrupolar interaction see, for instance, Refs. 19,20). We accept the form of the quadrupolar interaction of the electrostatic origin, which is free of any model assumptions. Thus, our consideration is confined to the Zeeman and quadrupolar interactions:

$$\mathcal{H} = \mathcal{H}_{\text{qd}} + \mathcal{H}_Z,$$

$$\mathcal{H}_{\text{qd}} = \sum_{\mathbf{r} \neq \mathbf{r}'} \sum_{i \dots n} \mathcal{A}_{ij, mn}(\mathbf{r} - \mathbf{r}') Q_{ij}(\mathbf{r}) Q_{mn}(\mathbf{r}'), \quad (12)$$

where $\mathcal{A}_{ij, mn}(\mathbf{r} - \mathbf{r}')$ is determined by the interaction $V_q(\mathbf{r} - \mathbf{r}')$ of two quadrupolar moments located at \mathbf{r} and \mathbf{r}' . The latter is given by

$$\begin{aligned}V_q(\mathbf{r}) &= \frac{1}{12r^5} \{ 2Q_{ij}(0)Q_{ij}(\mathbf{r}) - 20Q_{ij}(0)Q_{im}(\mathbf{r})n_jn_m \\ &\quad + 35Q_{ij}(0)Q_{mn}(\mathbf{r})n_in_jn_mn_n \}, \quad n_i = x_i/r.\end{aligned}\quad (13)$$

Thus we obtain from Eq. (13)

$$\begin{aligned}\mathcal{A}_{ij, mn}(\mathbf{r}) &= \frac{1}{24r^5} \{ (\delta_{im}\delta_{jn} + \delta_{in}\delta_{jm}) - 5(\delta_{im}n_jn_n \\ &\quad + \delta_{in}n_jn_m + \delta_{jm}n_in_n + \delta_{jn}n_in_m) \\ &\quad + 35n_in_jn_mn_n \}.\end{aligned}\quad (14)$$

Evident are the following properties of $\mathcal{A}_{ij, mn}$'s with respect to permutation of indices:

$$\mathcal{A}_{ij, mn} = \mathcal{A}_{ji, mn} = \mathcal{A}_{ij, nm} = \mathcal{A}_{mn, ij}.$$

TABLE I. Strength of the quadrupolar interaction at high symmetry points.

\mathbf{k}	$\mathcal{A}_{\mathbf{k}}^x$	$\mathcal{A}_{\mathbf{k}}^z$	$\mathcal{B}_{\mathbf{k}}^x$	$\mathcal{B}_{\mathbf{k}}^z$
$\frac{111}{222}$	-10.736	-10.736	1.789	1.789
$\frac{112}{220}$	-10.478	3.484	-0.581	2.909
$00\frac{1}{2}$	2.139	7.349	-0.357	-1.659
000	9.325	9.325	-1.554	-1.554

The diagonal elements of matrix $\|Q\|$ give rise to the order parameter which is transformed according to representation Γ_3 characterized by two components (τ_x, τ_z) of τ , while the off-diagonal elements are related to symmetry Γ_5 and are characterized by the vector μ . Keeping this in mind, we can rewrite \mathcal{H}_{qd} as follows:

$$\begin{aligned}\mathcal{H}_{\text{qd}} &= \sum_{\mathbf{r} \neq \mathbf{r}'} [\mathcal{A}_{\alpha\beta}(\mathbf{r} - \mathbf{r}') \tau_\alpha(\mathbf{r}) \tau_\beta(\mathbf{r}') \\ &\quad + \mathcal{B}_{ij}(\mathbf{r} - \mathbf{r}') \mu_i(\mathbf{r}) \mu_j(\mathbf{r}')],\end{aligned}\quad (15)$$

where the Greek indices α, β prescribe summation over x and z components only. The expressions for $\mathcal{A}_{\alpha\beta}$ and \mathcal{B}_{ij} are given in Appendix B. The Hamiltonian in Eq. (15) represents an evident separation of the orbitallike and spinlike parts.

The magnetic exchange interactions are not relevant for a theoretical analysis of the AFQ ordering in CeB₆. This applies to a major part of the phase diagram outside its low-temperature-and-weak-field part. The latter requires the RKKY- and Kondo-like interactions to be included.

III. TOWARDS QUADRUPOLEAR ORDERING

Taking the Fourier transform of the Hamiltonian (15), we arrive at its \mathbf{k} -diagonal form:

$$\mathcal{H}_{\text{qd}} = \sum_{\mathbf{k}} \{ \mathcal{A}^{\alpha\beta}[\mathbf{k}] \tau_{\mathbf{k},\alpha}^* \tau_{\mathbf{k},\beta} + \mathcal{B}^{ij}[\mathbf{k}] \mu_{\mathbf{k},i}^* \mu_{\mathbf{k},j} \}. \quad (16)$$

We use the notation $\mathcal{A}^{\alpha\beta}[\mathbf{k}]$ and $\mathcal{B}^{ij}[\mathbf{k}]$ for the Fourier transformed coupling constants at general \mathbf{k} . For high symmetry points of reciprocal space, such as [000], $[\frac{111}{222}]$, $[\frac{112}{220}]$, and $[00\frac{1}{2}]$, as well as along the cubic edge $[\frac{112}{22}\kappa]$, the Fourier transformed Hamiltonian (16) becomes completely diagonal:

$$\begin{aligned}\mathcal{H}_{\text{qd}} &= \sum_{\mathbf{k}} \{ \mathcal{A}_{\mathbf{k}}^x |\tau_{\mathbf{k},x}|^2 + \mathcal{A}_{\mathbf{k}}^z |\tau_{\mathbf{k},z}|^2 + \mathcal{B}_{\mathbf{k}}^x (|\mu_{\mathbf{k},x}|^2 + |\mu_{\mathbf{k},y}|^2) \\ &\quad + \mathcal{B}_{\mathbf{k}}^z |\mu_{\mathbf{k},z}|^2 \}.\end{aligned}\quad (17)$$

Table I shows the result of numerical calculations for the coefficients in units of Q_0^2/a^5 where a denotes the lattice constant. Let us estimate the order of such an energy unit. In doing so, we return to definition (8), and then, performing the radial and angular integrations, we get

$$Q_0 = -\frac{16}{35} e \langle r_f^2 \rangle.$$

Then the energy unit becomes $(e^2/a)(\langle r_f^2 \rangle/a^2)^2(16/35)^2$. For CeB₆, the lattice constant $a \approx 4 \text{ \AA}$, the f -electron radius $r_f \approx 0.4 \text{ \AA}$, the lattice Coulomb unit $e^2/a \approx 3 \text{ eV}$, and we

arrive at the Q_0 unit of order 1 K (cf., however, Ref. 21). From Table I one can see that the coefficients \mathcal{B}_k^α are small as compared to the dominant ones, \mathcal{A} 's. Additional smallness of the \mathcal{B} terms comes from the fact that the maximal value of μ_i^2 is 16/3 times smaller than the maximal value of τ_α^2 . Thus it seems appropriate to simplify the model by neglecting the \mathcal{B} terms and to employ the simplified version of \mathcal{H}_{qd} in its purely orbital τ form:

$$\mathcal{H}_{\text{orb}} = \sum_{\mathbf{r} \neq \mathbf{r}'} \sum_{\alpha\beta} \mathcal{A}_{\alpha\beta}(\mathbf{r}-\mathbf{r}') \tau_\alpha(\mathbf{r}) \tau_\beta(\mathbf{r}'). \quad (18)$$

According to Table I, the global energy minimum could be achieved at $\mathbf{k}=\mathbf{Q}$. Not only the high-symmetry points of reciprocal space, but also wave vectors of a general position have been checked numerically in order to identify \mathbf{Q} with the global energy minimum. It is necessary to emphasize that the energies at $\mathbf{k}=[\frac{1}{2}\frac{1}{2}0]$ and \mathbf{Q} are only slightly different. This is an indication of pronounced soft modes along the directions of cubic edges, i.e., $[\frac{1}{2}\frac{1}{2}\kappa]$, $[\frac{1}{2}\kappa\frac{1}{2}]$ and $[\kappa\frac{1}{2}\frac{1}{2}]$, $-1/2 \leq \kappa \leq 1/2$. Thus, competing AFQ patterns create fluctuations which should significantly decrease the AFQ-D transition temperature, as compared to the mean-field estimate. The wave vector \mathbf{Q} is consistent with the AFQ patterns which have been found experimentally by the Grenoble group.¹³

At the two points of reciprocal space, namely, $\mathbf{0}$ and \mathbf{Q} , we have $\mathcal{A}^{xx}=\mathcal{A}^{zz}$. Then the Fourier transform of \mathcal{H}_{orb} takes a planar form

$$\mathcal{A}_k(\tau_{-\mathbf{k},x}\tau_{\mathbf{k},x} + \tau_{-\mathbf{k},z}\tau_{\mathbf{k},z}).$$

In other high-symmetry points, $[\frac{1}{2}\frac{1}{2}0]$ and $[00\frac{1}{2}]$, \mathcal{H}_{orb} exhibits an easy-axis form with nonequal values of \mathcal{A}_k^x and \mathcal{A}_k^z . It is also valid for a general point of reciprocal space, but, in general, the off-diagonal component \mathcal{A}^{xz} is nonzero, and the easy axis should be different from either x axis or z axis.

It is worth noting that searching for the ground-state energy of the *classical* vector field $\boldsymbol{\tau}$ by using a Fourier transformation of Hamiltonian (18) (also known as the Luttinger-Tissa method) would be a standard procedure, if the Hamiltonian were invariant under the homogeneous $\boldsymbol{\tau}$ rotations. Nevertheless, although the rotational symmetry of \mathcal{H}_{orb} at $\mathbf{k}=[\frac{1}{2}\frac{1}{2}0]$ and $\mathbf{k}=[00\frac{1}{2}]$ is broken, the energy values listed in Table I are rigorous.

Magnetic ordering due to electric quadrupolar interactions

In this section we consider a quantum effect, namely the zero motion of the τ "spins" with respect to the AFQ background. In fact, when a decoupling procedure is applied to the \mathcal{B} terms in Eq. (15), we obtain the effective spinlike Hamiltonian:

$$\begin{aligned} \mathcal{H}_m &= \frac{3}{4} \sum_{\mathbf{r} \neq \mathbf{r}'} \mathcal{B}_{ij}(\mathbf{r}-\mathbf{r}') \langle \tau_y(\mathbf{r}) \tau_y(\mathbf{r}') \rangle \sigma_i(\mathbf{r}) \sigma_j(\mathbf{r}') \\ &= \sum_{\mathbf{r} \neq \mathbf{r}'} \tilde{\mathcal{B}}_{ij}(\mathbf{r}-\mathbf{r}') \sigma_i(\mathbf{r}) \sigma_j(\mathbf{r}'). \end{aligned} \quad (19)$$

τ_y does not enter the Hamiltonian (18); this is responsible for the formation of the orbital ordering. This would be a reason

for neglecting all the contributions caused by τ_y , including interaction (19), were it not for quantum fluctuations of $\boldsymbol{\tau}$. We put all the intermediate formulas, which determine our choice of the quantization axis, the spin-wave representation of $\boldsymbol{\tau}$'s, etc., into Appendix C.

In the spin-wave approximation Hamiltonian (18) becomes

$$\mathcal{H}_{\text{sw}} = \sum_{\mathbf{q}} \left(K_1(\mathbf{q}) b_{\mathbf{q}}^\dagger b_{\mathbf{q}} + \frac{1}{2} K_2(\mathbf{q}) (b_{-\mathbf{q}} b_{\mathbf{q}} + b_{\mathbf{q}}^\dagger b_{-\mathbf{q}}^\dagger) \right), \quad (20)$$

where

$$\begin{aligned} K_2(\mathbf{q}) &= \frac{1}{2} (\mathcal{A}^{zz}[\tilde{\mathbf{q}}] \sin^2 \phi + \mathcal{A}^{xx}[\tilde{\mathbf{q}}] \cos^2 \phi - \mathcal{A}^{xz}[\tilde{\mathbf{q}}] \sin 2\phi), \\ \tilde{\mathbf{q}} &= \mathbf{q} - \mathbf{Q}, \end{aligned} \quad (21)$$

and

$$K_1(\mathbf{q}) = K_2(\mathbf{q}) - \mathcal{A}_Q. \quad (22)$$

For definition of ϕ , see Appendix C. The energy gain $E_{\text{sw}}^{(0)}$, which occurs due to the zero motion of $\boldsymbol{\tau}$'s is a straightforward result of the Hamiltonian (20) diagonalization:

$$E_{\text{sw}}^{(0)} = -\frac{1}{2} \sum_{\mathbf{q}} (K_1 - \sqrt{K_1^2 - K_2^2}). \quad (23)$$

The correlation function

$$\langle \tau_y(0) \tau_y(\mathbf{r}) \rangle = \frac{1}{4} \sum_{\mathbf{q}} e^{i\mathbf{q}\mathbf{r}} \sqrt{(K_1 + K_2)/(K_1 - K_2)} \quad (24)$$

appears to be nonzero although it decays exponentially with distance r .

$E_{\text{sw}}^{(0)}$ is a periodic function of ϕ with periodicity $\pi/3$. In fact, using Eqs. (21)–(23) and definitions of \mathcal{A} 's given in Appendix B, one can rigorously prove that under the transformation $(q_x, q_y, q_z) \rightarrow (q_z, q_x, q_y)$ $K_1(\mathbf{q})$ and $K_2(\mathbf{q})$ remain unchanged, if ϕ is simultaneously shifted by $\pi/3$.

Numerical calculations show that $\phi=0, \pi/3, 2\pi/3$, etc., are related to equivalent minimums of $E_{\text{sw}}^{(0)}$. Using one of them, say, at $\phi=0$, we calculate the correlation functions (24) numerically. The sign of the first neighbor correlators is negative: $\langle \tau_y(0) \tau_y(\mathbf{a}_x) \rangle = \langle \tau_y(0) \tau_y(\mathbf{a}_y) \rangle \approx -0.0293$, $\langle \tau_y(0) \tau_y(\mathbf{a}_z) \rangle \approx -0.0058$. This is a reminder of the AFQ ordering. Among the second neighbors only $\langle \tau_y(0) \tau_y(\pm \mathbf{a}_x \pm \mathbf{a}_y) \rangle \approx -0.0082$ are not negligible, all others are much smaller. For the resulting coupling constants of Eq. (19) see Appendix B.

This curious mechanism which, in principle, leads to the effective magnetic interactions [see Eq. (19)], could be a reason for magnetic ordering at temperatures much smaller than T_Q , because, *first*, the \mathcal{B} coupling constants of Hamiltonian (16) are much less numerically than their \mathcal{A} counterparts, and, *second*, the additional smallness comes from the quantum fluctuations of τ_y 's. The low-temperature magnetism in CeB₆ is unlikely to be described by such an unusual mechanism. Such a mechanism would come into play only when all other magnetic interactions (mainly via conductivity electrons) were very weak.

IV. AF-QUADRUPOLAR-DISORDER TRANSITION

In this section we consider CeB₆ near the AFQ-D transition. For this we employ, following Ref. 14, the spherical model which is applicable to a system with well-pronounced soft modes. The purpose of this section is to determine (i) the shape of the AFQ-D transition line in the T - H phase diagram and (ii) the singularity of the specific heat along this line.

A. Spherical model and AFQ-D transition line

From the behavior of the specific heat anomaly^{8,9} (which is tiny in the weak magnetic field region) a strong short-range AFQ order should exist above $T_Q(H)$. A magnetic field suppresses the fluctuations and makes $T_Q(H)$ higher. In order to pick up these features, we go beyond the mean-field approximation for Hamiltonian $\mathcal{H}_Z + \mathcal{H}_{\text{orb}}$. The first step in this direction will be generalization of the spherical model for two spins, $\boldsymbol{\sigma}$ and $\boldsymbol{\tau}$. For taking into account the quantum effects, we impose the constraints $\langle \boldsymbol{\sigma}^2(\mathbf{r}) \rangle = 3/4$ and $\langle \boldsymbol{\tau}^2(\mathbf{r}) \rangle = 1/2$. The latter would be equal to $3/4$ were it not for redundancy of the τ_y variable. Note that, as shown in Ref. 22, the decoupling of fluctuations in the spin-1/2 Heisenberg model leads to the spherical model with the constraint $\langle \boldsymbol{\sigma}^2(\mathbf{r}) \rangle = 3/4$. Now the partition function reads

$$\mathcal{Z} = \prod_{\mathbf{r}} \int_{-\infty}^{\infty} d\boldsymbol{\sigma}(\mathbf{r}) \int_{-\infty}^{\infty} d\boldsymbol{\tau}(\mathbf{r}) \exp\beta\{\lambda_{\sigma}[3/4 - \boldsymbol{\sigma}^2(\mathbf{r})] + \lambda_{\tau}[1/2 - \boldsymbol{\tau}^2(\mathbf{r})] - (\mathcal{H}_{\text{orb}} + \mathcal{H}_Z)\}, \quad (25)$$

where the spherical conditions

$$\partial\mathcal{F}/\partial\lambda_{\tau} = \partial\mathcal{F}/\partial\lambda_{\sigma} = 0 \quad (\mathcal{F} = -T \ln\mathcal{Z}),$$

$$-\mathcal{F} = \frac{3}{4}\lambda_{\sigma} + \frac{1}{2}\lambda_{\tau} + \left(\frac{7}{8}\right)^2 \left(z + \frac{z^2}{\lambda_{\tau} + \mathcal{A}_0 - z}\right) + \frac{3}{2}T \ln \frac{\pi T}{\lambda_{\sigma}} + \frac{T}{2} \int \frac{d^3k}{(2\pi)^3} \ln \frac{(\pi T)^2}{(\lambda_{\tau} + \mathcal{A}^{zz}[\mathbf{k}] - z)(\lambda_{\tau} + \mathcal{A}^{xx}[\mathbf{k}]) - (\mathcal{A}^{xz}[\mathbf{k}])^2}, \quad (26)$$

where

$$z = \left(\frac{8}{7}\right)^2 \frac{(\mu_B H)^2}{\lambda_{\sigma}}. \quad (27)$$

Two equations,

$$\frac{1}{2} - \left(\frac{7}{8}\right)^2 \frac{z^2}{(\lambda_{\tau} + \mathcal{A}_0 - z)^2} = \frac{T}{2} \int \frac{d^3k}{(2\pi)^3} \frac{2\lambda_{\tau} + \mathcal{A}^{zz}[\mathbf{k}] + \mathcal{A}^{xx}[\mathbf{k}] - z}{(\lambda_{\tau} + \mathcal{A}^{zz}[\mathbf{k}] - z)(\lambda_{\tau} + \mathcal{A}^{xx}[\mathbf{k}]) - (\mathcal{A}^{xz}[\mathbf{k}])^2} \quad (28)$$

and

$$\frac{3}{4} - \left(\frac{7}{8}\right)^2 \frac{z}{\lambda_{\sigma}} - \left(\frac{7}{8}\right)^2 \frac{z^2}{\lambda_{\sigma}(\lambda_{\tau} + \mathcal{A}_0 - z)} \left(2 + \frac{z}{\lambda_{\tau} + \mathcal{A}_0 - z}\right) - \frac{3T}{2\lambda_{\sigma}} = \frac{T}{2} \frac{z}{\lambda_{\sigma}} \int \frac{d^3k}{(2\pi)^3} \frac{\lambda_{\tau} + \mathcal{A}^{xx}[\mathbf{k}]}{(\lambda_{\tau} + \mathcal{A}^{zz}[\mathbf{k}] - z)(\lambda_{\tau} + \mathcal{A}^{xx}[\mathbf{k}]) - (\mathcal{A}^{xz}[\mathbf{k}])^2}, \quad (29)$$

are valid for the D phase and determine λ_{σ} and λ_{τ} as functions of T and H , through which the physical quantities can be then expressed. The integrals in the right-hand side of Eqs. (28) and (29) are not of that simple form as the Watson integral, which appears in the spherical model treatment of the 3D ferromagnet, but let us call them generalized Watson integrals. The AFQ-D transition line corresponds to the values of λ_{τ} at which the denominator of the generalized Watson integrals turns zero at $\mathbf{k} = \mathbf{Q}$. Taken at the critical value

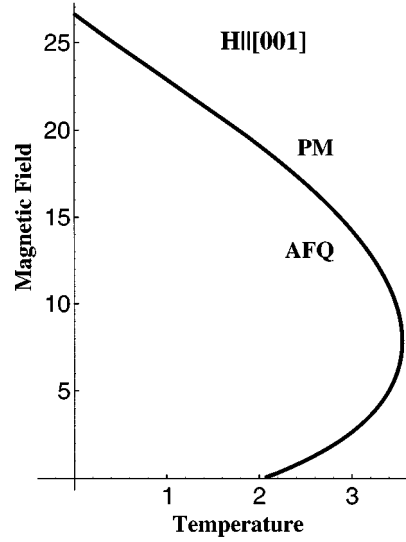


FIG. 5. The line of the AFQ-D phase transition according to Eqs. (26)–(27). Units for T and H are discussed in the text.

which control the constraints, should be satisfied by an appropriate choice of λ_{τ} and λ_{σ} . Gaussian integration over $\boldsymbol{\sigma}(\mathbf{r})$ and $\boldsymbol{\tau}(\mathbf{r})$ in Eq. (25) is straightforward; that allows us to derive the free energy \mathcal{F} of the spherical model.

For definiteness, we inspect the particular case of $\mathbf{H}||[001]$: This orientation is expected to favor the reentrance of the AFQ-D transition line at smaller H as compared to other orientations. The singularities on the AFQ-D transition line, as well as its shape, will be examined as temperature decreasing, i.e., from the side of the D phase.

Performing the routine calculations, which are given in Appendix D, we get [cf. Eqs. (D2),(D3),(D5)]

$$\lambda_\tau^{(c)}(z) = |\mathcal{A}_Q| + z, \quad (30)$$

Eqs. (28) and (29) determine $T_Q(H)$. This line is depicted in Fig. 5.

At zero magnetic field, $\lambda_\sigma = 2T_Q$ and $T_Q = [W_1(z=0)]^{-1}$, as seen from Eqs. (29) and (28), respectively. We denote the first generalized Watson integral [see Eq. (28)] taken along the transition line by $W_1(z)$. It can be written now as

$$W_1(z) = \int \frac{d^3k}{(2\pi)^3} \frac{2|\mathcal{A}_Q| + \mathcal{A}^{zz}[\mathbf{k}] + \mathcal{A}^{xx}[\mathbf{k}] + z}{(|\mathcal{A}_Q| + \mathcal{A}^{xx}[\mathbf{k}] + z)(|\mathcal{A}_Q| + \mathcal{A}^{zz}[\mathbf{k}]) - (\mathcal{A}^{xz}[\mathbf{k}])^2}. \quad (31)$$

In order to estimate the importance of fluctuations, we can compare the spherical model and mean-field results for T_Q . The mean-field approach yields $T_Q^{\text{MF}}(H=0) = |\mathcal{A}_Q|/2 = 5.37$, and $T_Q(H)$ decreases monotonically with increasing H .¹⁴

An important property of $T_Q(H)$ should be mentioned in connection with Fig. 5 (cf. Fig. 3), i.e., $T_Q(H)$ grows *linearly* with H at not very high magnetic fields. This feature is consistent with experimental findings. Mathematically, this behavior follows from the properties of the generalized Watson integrals: their expansions in a small parameter z are $c_0^{(i)} - c_1^{(i)}\sqrt{z}$, where all four values of c are positive. Then, because in the leading order $T_Q(H) - T_Q(0) \approx [W_1(0) - W_1(z)]/[W_1(0)]^2$, as it follows from Eq. (28), the weak-field behavior of T_Q becomes clearly understood. To complete this proof, let us represent $[W_1(z) - W_1(0)]$ as follows:

$$W_1(0) - W_1(z) = z \int \frac{d^3k}{(2\pi)^3} \frac{(|\mathcal{A}_Q| + \mathcal{A}^{zz}[\mathbf{k}])^2 + (\mathcal{A}^{xz}[\mathbf{k}])^2}{\mathcal{D}([\mathbf{k}]; z)\mathcal{D}([\mathbf{k}]; z=0)}, \quad (32)$$

which is positive. We denote the denominator of integral (31) by $\mathcal{D}([\mathbf{k}]; z)$. At $z=0$, integral in Eq. (32) becomes singular at small $\delta\mathbf{k} = \mathbf{k} - \mathbf{Q}$. In fact, the numerator behaves as $\delta\mathbf{k}^4$, whereas the denominator $\propto \delta\mathbf{k}^8$. The integral would diverge as $|\delta\mathbf{k}|^{-1}$ were it not for the cutoff at $|\delta\mathbf{k}|^2 \sim z$. Thus we arrive at $W_1(0) - W_1(z) \propto \sqrt{z}$.

It is worth noting, that the spherical model is a reasonable tool for picking up strong fluctuations. However, if fluctuations are effectively suppressed, as is the case in high magnetic fields, the spherical model performs less satisfactorily.

B. Specific heat

Here we confine our consideration to the vicinity of the AFQ-D transition line and magnetic fields weak as compared to T_Q ($\mu_B H \ll T_Q$). The equations which determine thermodynamic behavior are Eqs. (28) and (29), where we can neglect all high order terms in H (H^n with $n \geq 2$). Using the spherical conditions ($\partial\mathcal{F}/\partial\lambda_\sigma = \partial\mathcal{F}/\partial\lambda_\tau = 0$), one can obtain for the entropy ($S = -\partial\mathcal{F}/\partial T$):

$$S = \frac{3}{2} \ln \frac{\pi T}{\lambda_\sigma} + \frac{5}{2} + \frac{1}{2} \int \frac{d^3k}{(2\pi)^3} \ln \frac{(\pi T)^2}{(\lambda_\tau + \mathcal{A}^{zz}[\mathbf{k}] - z)(\lambda_\tau + \mathcal{A}^{xx}[\mathbf{k}]) - (\mathcal{A}_{xz}[\mathbf{k}])^2}. \quad (33)$$

The specific heat at constant field, $C_H = T(\partial S/\partial T)_H$, is now determined as follows:

$$C_H = \frac{5}{2} - \frac{T}{2} \frac{d\lambda_\tau}{dT} \int \frac{d^3k}{(2\pi)^3} \frac{2\lambda_\tau + \mathcal{A}^{zz}[\mathbf{k}] + \mathcal{A}^{xx}[\mathbf{k}] - z}{(\lambda_\tau + \mathcal{A}^{zz}[\mathbf{k}] - z)(\lambda_\tau + \mathcal{A}^{xx}[\mathbf{k}]) - (\mathcal{A}_{xz}[\mathbf{k}])^2} - \frac{3}{2} \frac{T}{\lambda_\sigma} \frac{d\lambda_\sigma}{dT} - \frac{Tz}{2\lambda_\sigma} \frac{d\lambda_\sigma}{dT} \int \frac{d^3k}{(2\pi)^3} \frac{\lambda_\tau + \mathcal{A}^{xx}[\mathbf{k}]}{(\lambda_\tau + \mathcal{A}^{zz}[\mathbf{k}] - z)(\lambda_\tau + \mathcal{A}^{xx}[\mathbf{k}]) - (\mathcal{A}_{xz}[\mathbf{k}])^2}. \quad (34)$$

With using Eqs. (28) and (29) we can transform Eq. (34) into the simple form

$$C_H = \frac{5}{2} - \frac{1}{2} \frac{d\lambda_\tau}{dT} - \frac{3}{4} \frac{d\lambda_\sigma}{dT}. \quad (35)$$

Let us consider a fixed magnetic field and $T > T_Q(H)$, i.e., $T = T_Q(H) + \delta T$. At $\delta T \ll T_Q$, $\lambda_\tau = |\mathcal{A}_Q| + z + \delta\lambda_\tau$ is supposed to be slightly different from $\lambda_\tau^{(c)}(z)$ [see Eq. (30)]. In order to find out $\delta\lambda_\tau(\delta T)$ we return to Eq. (28) which takes the following form at $z \ll T_Q$:

$$\frac{1}{2} = \frac{1}{2} [T_Q(H) + \delta T] [W_1(z) - \sqrt{\delta\lambda_\tau} w(z/\delta\lambda_\tau; \delta\lambda_\tau)], \quad (36)$$

where w is positive:

$$w(z/\delta\lambda_\tau; \delta\lambda_\tau) = \frac{1}{\sqrt{\delta\lambda_\tau}} \left[W_1(z) - \int \frac{d^3k}{(2\pi)^3} \frac{2|\mathcal{A}_Q| + \mathcal{A}^{zz}[\mathbf{k}] + \mathcal{A}^{xx}[\mathbf{k}] + 2\delta\lambda_\tau + z}{(|\mathcal{A}_Q| + \mathcal{A}^{xx}[\mathbf{k}] + \delta\lambda_\tau + z)(|\mathcal{A}_Q| + \mathcal{A}^{zz}[\mathbf{k}] + \delta\lambda_\tau) - (\mathcal{A}^{xz}[\mathbf{k}])^2} \right]. \quad (37)$$

In Fig. 6 w is depicted as function of $\delta\lambda_\tau$ for three values of the ratio $z/\delta\lambda_\tau$. It can be remarkably well approximated to the form $w_0(\delta\lambda_\tau)[1 + \alpha(\delta\lambda_\tau)\sqrt{z/\delta\lambda_\tau}]^{-1}$, where $w_0(x) = w(0;x)$ (see the upper curve in Fig. 6) and $\alpha(x)$ are both weakly dependent functions of the argument. For example, $\alpha(0) \approx 0.7$ and $\alpha(1) \approx 1.15$. Note, that α and $wT_Q^{3/2}$ are dimensionless quantities ($w_0T_Q^{3/2} \sim 1$). Thus, in the leading order, when $\delta\lambda_\tau \ll z$, which is equivalent to $\delta T \ll \mu_B H$, we obtain

$$\delta\lambda_\tau \approx \frac{\alpha(0)}{w_0(0)} \frac{W_1(z)}{T_Q} \delta T \sqrt{z}$$

and, because $W_1(z) \approx T_Q^{-1}$,

$$\frac{d\lambda_\tau}{dT} \approx \frac{\alpha(0)}{w_0(0)} \frac{1}{T_Q^2} \sqrt{z}. \quad (38)$$

In accordance with Eq. (29)

$$\lambda_\sigma = 2T + O[(\mu_B H)^2/T_Q]. \quad (39)$$

Therefore, in the leading order in H one can obtain from Eqs. (35), (38), and (39):

$$\lim_{\delta T \rightarrow +0} C_H = 1 - \frac{4}{7} \frac{\alpha(0)}{w_0(0)} \frac{1}{T_Q^2} \frac{\mu_B H}{\sqrt{2T_Q}}. \quad (40)$$

Below $T_Q(H)$ λ_τ does not depend anymore on δT and remains equal to $|\mathcal{A}_Q| + z$. Thus, we get

$$\lim_{\delta T \rightarrow -0} C_H = 1, \quad (41)$$

which, together with Eq. (40), determines the specific heat jump, increasing linearly with H .

At $T_Q \gg \delta T \gg \mu_B H$, i.e., beyond a narrow vicinity of the transition line, we arrive at C_H , decreasing linearly with δT :

$$C_H = 1 - T_Q^{-1} w_0^{-1} \delta T.$$

V. WELL-ISOLATED Γ_8 LEVELS: A SINGLE f -HOLE CONFIGURATION

Zeeman and quadrupolar interactions

Now we deal with the following quantum numbers: $\mathcal{J} = 7/2$, $S = 1/2$, and $L = 3$. In the crystal field of cubic symmetry the eightfold multiplet splits into the Γ_8 quartet and two doublets, Γ_6 and Γ_7 . If the crystal field Hamiltonian

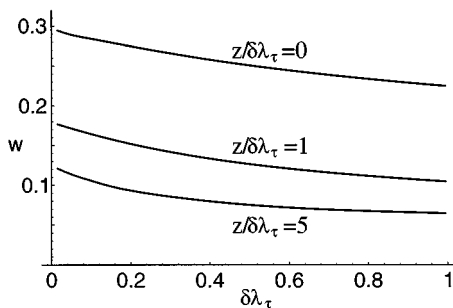


FIG. 6. $w(z/\delta\lambda_\tau; \delta\lambda_\tau)$ as function of $\delta\lambda_\tau$ [Eq. (37)].

allows the quartet to be realized as a well-isolated ground-state level, then we confine our consideration to the following set of wave functions:

$$\begin{aligned} \psi_{1,\pm} &= \pm \sqrt{7/12} |\mp 7/2\rangle \mp \sqrt{5/12} |\pm 1/2\rangle, \\ \psi_{2,\pm} &= \mp \frac{1}{2} |\pm 5/2\rangle \mp \frac{\sqrt{3}}{2} |\mp 3/2\rangle. \end{aligned} \quad (42)$$

Listed below in units of μ_B are the nonzero matrix elements of M_z , M_+ , and M_- :

$$\begin{aligned} \langle \psi_{1,+} | M_z | \psi_{1,+} \rangle &= -\langle \psi_{1,-} | M_z | \psi_{1,-} \rangle = -44/21; \\ \langle \psi_{2,+} | M_z | \psi_{2,+} \rangle &= -\langle \psi_{2,-} | M_z | \psi_{2,-} \rangle = -4/7; \\ \langle \psi_{2,-} | M_+ | \psi_{1,+} \rangle &= \langle \psi_{1,+} | M_- | \psi_{2,-} \rangle = -16/(7\sqrt{3}); \\ \langle \psi_{2,+} | M_- | \psi_{1,-} \rangle &= \langle \psi_{1,-} | M_+ | \psi_{2,+} \rangle = -16/(7\sqrt{3}); \\ \langle \psi_{1,-} | M_- | \psi_{1,+} \rangle &= \langle \psi_{1,+} | M_+ | \psi_{1,-} \rangle = -40/21; \\ \langle \psi_{2,-} | M_- | \psi_{2,+} \rangle &= \langle \psi_{2,+} | M_+ | \psi_{2,-} \rangle = -24/7. \end{aligned} \quad (43)$$

All these matrix elements are in accordance with the operator expression:

$$M_i = -\frac{8}{3} \mu_B \sigma_i \left(1 + \frac{8}{7} T_i \right), \quad i = x, y, z. \quad (44)$$

Note that the only difference between Eqs. (44) and (5) is the coefficient ($-8/3$ instead of 2).

Now let us determine the matrix $\|Q\|$. For the unit, we take

$$Q_0 = \langle \psi_{1,\sigma} | Q_{zz} | \psi_{1,\sigma} \rangle.$$

The diagonal components of the quadrupolar moment have the same nonzero matrix elements as in Eq. (9), whereas the matrix elements of the off-diagonal components are six times larger than the corresponding elements of Eq. (10). Thus, the form of $\|Q\|$ is the same as in Eq. (11), but the off-diagonal ‘‘vectors,’’ which transform in accordance with Γ_5 , are defined now as $\boldsymbol{\mu} = 3\sqrt{3}\tau_y \boldsymbol{\sigma}$. This circumstance makes the problem of quadrupolar ordering less transparent as in the single f -electron case: The part of \mathcal{H}_{qd} [see Eq. (15)], which reflects the μ - μ interactions, becomes as important as the τ - τ part.

There are a few compounds of cubic symmetry, based on the single f -hole ions, which can be the candidates to realize the Γ_8 quadrupolar ordering. Among them we would mention YbB_{12} (Ref. 23) and TmTe .²⁴ There is another important difference between these face-cubic centered compounds and CeB_6 (recall, that Ce ions are arranged in a simple cubic lattice). Namely, fcc compounds do not exhibit such pronounced soft modes as in the simple cubic case. It is not our purpose to give a detailed analysis of the fcc situation in the framework of the realistic quadrupolar interaction (13). We mention, however, that the ground state of the analog of \mathcal{H}_{orb} [see Eq. (18)] is of the AFQ-type, which is related to the high-symmetry points ($\mathbf{Q}_x, \mathbf{Q}_y, \mathbf{Q}_z$) of the Brillouin zone boundaries (see Fig. 7): $E(\mathbf{k} = \mathbf{Q}_i) \approx -8.85$ at them. The order parameter at, say $\mathbf{k} = \mathbf{Q}_z$, corresponds to the Ising-like

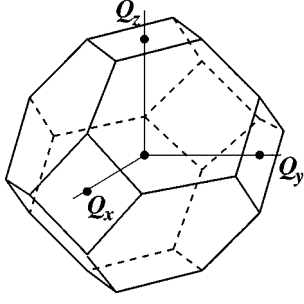


FIG. 7. The first Brillouin zone of reciprocal space of the fcc structure.

symmetry with $\langle \tau_z \rangle = 0$ and $\langle \tau_x \rangle$, altering the sign from layer to layer. The direction of low-lying excitations coincides with $[001]$, but the mode is not a soft one: $E(\mathbf{k}=\mathbf{0}) - E(\mathbf{k}=\mathbf{Q}) \approx 3.99$.

VI. DISCUSSION AND CONCLUSIONS

The problem of quadrupolar ordering in CeB₆ seems to be well defined provided we confine our attention to the Zeeman energy and direct quadrupolar interactions. The unusual form of these Zeeman and quadrupolar terms owes to the well-isolated Γ_8 quartet. Instead of dealing with Stevens operators, it is more convenient to introduce the spinlike, σ , and orbital-like, τ , operators. However, in the low-temperature and weak-field region CeB₆ undergoes the magnetic phase transition (see Fig. 2), which results in the appearance of complicated magnetic structures. For their explanation it is insufficient to restrict ourselves to the above-mentioned interactions only, but indirect interactions via conductivity electrons start playing an important role. Magnetic domains of different orientations have been identified in neutron diffraction experiments²⁵ for magnetic fields applied along $[111]$, $[110]$, and $[001]$. However the interpretation of neutron experiments^{13,15,25} occurs to be contradictory to recent μ SR measurements.¹⁷ As for the AFQ ordered state, the neutron NMR results are still in disagreement: The triple- \mathbf{k} structure has been proposed by Takigawa *et al.*,¹¹ whereas in all the neutron experiments the \mathbf{Q} modulation has been reported ($\mathbf{Q} = [\frac{1}{2}\frac{1}{2}\frac{1}{2}]$). These two interpretations are mutually exclusive. Unfortunately, Ref. 11 is a short paper with not many details; we mention a few of them to show a sig-

nificant difference of the triple- \mathbf{k} ($\mathbf{q}_1 = [\frac{1}{2}00]$, $\mathbf{q}_2 = [0\frac{1}{2}0]$, $\mathbf{q}_3 = [00\frac{1}{2}]$) and \mathbf{Q} modulated structures.

For the modulated component of magnetization $\mathbf{m}(\mathbf{r})$ the following equation has been proposed in Ref. 11:

$$\mathbf{m}(\mathbf{r}) = (-1)^\ell \mathbf{m}_1 + (-1)^m \mathbf{m}_2 + (-1)^n \mathbf{m}_3, \quad (45)$$

where $\mathbf{r} = (\ell, m, n)$, and the polarization vectors depend on the magnetic field direction $[\mathbf{H}] = (\cos\theta_1, \cos\theta_2, \cos\theta_3)$ through the equations

$$\mathbf{m}_1 = m_1(\theta_1)(\cos\theta_1, -\cos\theta_2, -\cos\theta_3),$$

$$\mathbf{m}_2 = m_2(\theta_2)(-\cos\theta_1, \cos\theta_2, -\cos\theta_3),$$

$$\mathbf{m}_3 = m_3(\theta_3)(-\cos\theta_1, -\cos\theta_2, \cos\theta_3). \quad (46)$$

An important property of $\{m_i\}$ is that $m_i(\pi/2) = 0$. The form of Eqs. (45)–(46) is not transparent, it is easier to illustrate them with a couple of examples.

In the first example $\mathbf{H} \parallel [001]$, which leads to $\theta_1 = \theta_2 = \pi/2$, hence, $m_1 = m_2 = 0$. This corresponds to a degeneracy of the triple- \mathbf{k} structure, whose realization now is a single- \mathbf{k} structure. According to Eq. (46) the modulated component of magnetization is arranged as shown in Fig. 8(a). Our theoretical description results in the arrangement shown in Fig. 8(b).

In the second example $\mathbf{H} \parallel [110]$, and $\theta_3 = \pi/2$, $\theta_1 = \theta_2 = \pi/4$ lead to $m_3 = 0$, $m_1 = m_2$. This degeneracy corresponds to a double- \mathbf{k} structure. Figures 9(a) and 9(b) are the NMR and theoretical interpretations, respectively. Note, that the Fig. 9(a) pattern reproduces itself under any translation along $[001]$, while \mathbf{m} 's of Fig. 9(b) alter the sign under the translation by the elementary lattice constant.

The preliminary μ SR results¹⁷ contradict both neutron and NMR measurements.

A critical experiment seems to be not difficult to achieve. It is connected with the x-ray structural measurements at zero magnetic field. The translational electric symmetry of the Ce lattice is broken below T_Q : although all the electric charges of Ce ions are equal to each other, the modulated component of the quadrupolar moment should contribute to the Bragg reflections at the transferred wave vectors of the $[\frac{1}{2}\frac{1}{2}\frac{1}{2}]$ type. This would be a weak effect, caused by only one electron of the total number Z . However, instead of an usual x-ray tech-

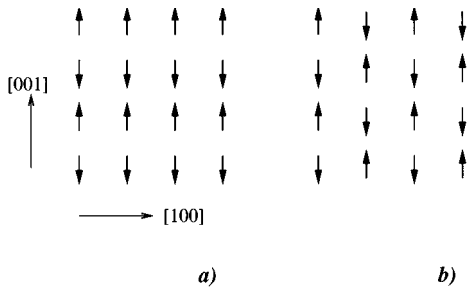


FIG. 8. Arrangement of staggered magnetization for magnetic field applied along $[001]$; (a) NMR interpretation (Ref. 11); (b) \mathbf{Q} -modulated structure.

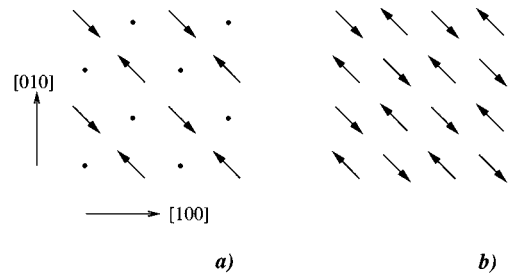


FIG. 9. Arrangement of staggered magnetization for magnetic field applied along $[110]$; (a) NMR interpretation (Ref. 11); (b) \mathbf{Q} -modulated structure.

nique it would be possible to use synchrotron facilities for finding the \mathbf{Q} or triple- \mathbf{k} modulated structure (or something different from these two). Note, that the zero field experiment is more instructive because it allows to avoid the sec-

ondary effects in nonzero fields, i.e., formations of magnetically modulated structures. To complete this x-ray discussion we give the on-site form-factor *operator* which is calculated over the set $\{\psi_{\ell,\sigma}\}$ and related to the f electron *only*:

$$f(\mathbf{q}) = \langle j_0 \rangle + \frac{1}{2} \langle j_4 \rangle P_4(z_{\mathbf{q}}) + \frac{1}{7} \tau_z(\mathbf{r}) [16 \langle j_2 \rangle P_2(\cos \theta_{\mathbf{q}}) - 5 \langle j_4 \rangle P_4(z_{\mathbf{q}})] + \frac{1}{7\sqrt{3}} \tau_x(\mathbf{r}) [8 \langle j_2 \rangle P_2^2(z_{\mathbf{q}}) + \langle j_4 \rangle P_4^2(z_{\mathbf{q}})] \cos 2\phi_{\mathbf{q}},$$

$$z_{\mathbf{q}} = \cos \theta_{\mathbf{q}}.$$

$\theta_{\mathbf{q}}$ and $\phi_{\mathbf{q}}$ denote the spherical coordinates of \mathbf{q} relative to the z axis. $P_l^m(z)$ are associated Legendre polynomials. Detailed calculations in connection with a concrete x-ray (synchrotron) experiment will be published elsewhere.

The experimental technique which is associated with the so-called third order paramagnetic susceptibility²⁶ can be also used for probing the quadrupolar ordering in CeB₆. However, it cannot yield information about the microscopic arrangement of quadrupolar moments. This method is based on the extraction of the H^3 terms from $M(H)$, when H is small. For our problem, the average magnetization can be written as

$$\bar{M}_{\alpha} = -\frac{1}{6T^3} \frac{1}{N_{\mathbf{r}_1 \dots \mathbf{r}_4}} \sum_{\mathbf{r}_1 \dots \mathbf{r}_4} \{ \langle M_{\alpha}(\mathbf{r}_1) M_{\beta}(\mathbf{r}_2) M_{\mu}(\mathbf{r}_3) M_{\nu}(\mathbf{r}_4) \rangle - 3 \langle M_{\alpha}(\mathbf{r}_1) M_{\beta}(\mathbf{r}_2) \rangle \langle M_{\mu}(\mathbf{r}_3) M_{\nu}(\mathbf{r}_4) \rangle \} H_{\beta} H_{\mu} H_{\nu}. \quad (47)$$

For further transformations in Eq. (47), we imply that, *first*, all the magnetic fluctuations are much smaller as compared to the quadrupolar fluctuations in the AFQ phase (at least near T_Q), *second*, the diagonal components of the quadrupolar moment are responsible for ordering below T_Q . Then, using the Wigner-Eckhart theorem we can decouple Eq. (47) according to the following scheme:

$$M_{\alpha}(\mathbf{r}) M_{\beta}(\mathbf{r}') \rightarrow \left(\frac{7}{6}\right)^2 \mu_B^2 \mathcal{J}_{\alpha}(\mathbf{r}) \mathcal{J}_{\beta}(\mathbf{r}) \delta_{\mathbf{r},\mathbf{r}'} \rightarrow \left(\frac{7}{6}\right)^2 \mu_B^2 Q_0^{-1} [T_{\alpha}(\mathbf{r}) + \mathcal{J}(\mathcal{J}+1)/3] \delta_{\alpha\beta} \delta_{\mathbf{r},\mathbf{r}'},$$

and arrive at the following equation $\bar{M}_{\alpha} = \bar{M}_{\alpha}^{(0)} + \bar{M}_{\alpha}^{(1)}$, where

$$\bar{M}_{\alpha}^{(1)} = -\frac{\mu_B^4}{2T^3} \left(\frac{7}{6}\right)^4 \frac{1}{N} \sum_{\mathbf{r}' \neq \mathbf{r}} \frac{1}{Q_0^2} \sum_{\mu} [\langle T_{\alpha}(\mathbf{r}) T_{\mu}(\mathbf{r}') \rangle - \langle T_{\alpha}(\mathbf{r}) \rangle \langle T_{\mu}(\mathbf{r}') \rangle] H_{\alpha} H_{\mu}^2, \quad (48)$$

$$\bar{M}_{\alpha}^{(0)} = -\frac{\mu_B^4}{6T^3} \left(\frac{7}{6}\right)^4 \frac{1}{N} \sum_{\mathbf{r}} \sum_{\beta, \mu, \nu} H_{\beta} H_{\mu} H_{\nu} [\langle \mathcal{J}_{\alpha}(\mathbf{r}) \mathcal{J}_{\beta}(\mathbf{r}) \mathcal{J}_{\mu}(\mathbf{r}) \mathcal{J}_{\nu}(\mathbf{r}) \rangle - \langle \mathcal{J}_{\alpha}(\mathbf{r}) \mathcal{J}_{\beta}(\mathbf{r}) \rangle \langle \mathcal{J}_{\mu}(\mathbf{r}) \mathcal{J}_{\nu}(\mathbf{r}) \rangle - \langle \mathcal{J}_{\alpha}(\mathbf{r}) \mathcal{J}_{\mu}(\mathbf{r}) \rangle \langle \mathcal{J}_{\beta}(\mathbf{r}) \mathcal{J}_{\nu}(\mathbf{r}) \rangle - \langle \mathcal{J}_{\alpha}(\mathbf{r}) \mathcal{J}_{\nu}(\mathbf{r}) \rangle \langle \mathcal{J}_{\beta}(\mathbf{r}) \mathcal{J}_{\mu}(\mathbf{r}) \rangle]. \quad (49)$$

Equation (48) includes the irreducible correlators of τ_x and τ_z . The on-site irreducible correlator enters Eq. (49). The average of four \mathcal{J} 's can be reduced to a linear-in- τ expectation value which disappears upon summation over \mathbf{r} . The $\langle \mathcal{J}\mathcal{J} \rangle^2$ terms of Eq. (49) result in the contribution $\propto \langle \tau \rangle^2$, which should produce a kink in a dependence $\chi^{(3)}$ versus T at T_Q .

The AFQ-D transition line was recently measured in fields up to 18 T.¹⁶ In spite of its tendency to reenter, this curve still displays the monotonic $T_Q(H)$ behavior. An optimistic theoretical prediction is ~ 25 – 30 T for the field at which the reentrance could start and ~ 80 T for the zero-temperature critical field. The current experimental facilities are enough to examine the field region around 25–30 T.

Although many experimental results can be explained by the present theory (see also Refs. 14,27), still there remain a few puzzling facts. Among them we would mention the AFQ-D transition line whose experimental shape is practically independent on the field orientation, [001], [110], or

[111]. Probably, such behavior could be ascribed to an unusual anisotropy of the Zeeman energy. In fact, if we consider an isolated Γ_8 ion, its ground-state energy depends on the magnetic field direction as follows:

$$E_{\text{g.s.}} = -\frac{\mu_B H}{7} \sqrt{65 + 4 \sqrt{270(n_x^4 + n_y^4 + n_z^4) - 74}}, \quad (50)$$

that is -11 , -9.81 , and -9 (in units $\mu_B H/7$) for orientations [001], [110], and [111], respectively. For magnetic field of a general orientation, the vector of magnetization in such a paramagnetic state does not follow the same direction. In this connection, the experiments with diluted compounds La_{1-x}Ce_xB₆ could provide important information, if the crystal field still favors the Γ_8 ground state.

From the theoretical point of view it should be interesting to understand the symmetry and a microscopic origin of the magnetic interactions which govern the properties of the system at low temperatures.

TABLE II. The operator forms for transformations $|\ell, \sigma\rangle \rightarrow |\ell', \sigma'\rangle$.

	$ 1, +\rangle$	$ 1, -\rangle$	$ 2, +\rangle$	$ 2, -\rangle$
$ 1, +\rangle$	$(\frac{1}{2} + \tau_z)(\frac{1}{2} + \sigma_z)$	$(\frac{1}{2} + \tau_z)\sigma_-$	$\tau_-(\frac{1}{2} + \sigma_z)$	$\tau_- \sigma_-$
$ 1, -\rangle$	$(\frac{1}{2} + \tau_z)\sigma_+$	$(\frac{1}{2} + \tau_z)(\frac{1}{2} - \sigma_z)$	$\tau_- \sigma_+$	$\tau_-(\frac{1}{2} - \sigma_z)$
$ 2, +\rangle$	$\tau_+(\frac{1}{2} + \sigma_z)$	$\tau_+ \sigma_-$	$(\frac{1}{2} - \tau_z)(\frac{1}{2} + \sigma_z)$	$(\frac{1}{2} - \tau_z)\sigma_-$
$ 2, -\rangle$	$\tau_+ \sigma_+$	$\tau_+(\frac{1}{2} - \sigma_z)$	$(\frac{1}{2} - \tau_z)\sigma_+$	$(\frac{1}{2} - \tau_z)(\frac{1}{2} - \sigma_z)$

ACKNOWLEDGMENTS

I take the opportunity to thank A. Lacerda and M. Torikachvili for sending me the experimental data prior to their publication. When making this work I had fruitful and enlightening discussions with P. Burlet, H. Capellmann, Yu. Chernenkov, J. Flouquet, T. Kasuya, V. Mineev, P. Morin, E. Müller-Hartmann, V. Plakhty, L.-P. Regnault, J. Schweizer, and C. Vettier. It is my pleasure to thank M. Burgess for linguistic comments. This work has been done

during my stay at CEN/CNRS in Grenoble, in accordance with the program of the Ecole Normale Supérieure–Landau Institute cooperation.

APPENDIX A

In order to construct the operator expressions for \mathbf{M} , as well as for Q_{ij} , we employ Table II. It shows the operator connection between all four possible states. Using matrix elements (4) in combination with Table II one can obtain for $M_x = (M_+ + M_-)/2$, for example,

$$\begin{aligned}
 M_x &= \frac{\mu_B}{2} \left(\frac{4\sqrt{3}}{7} (\tau_- \sigma_- + \tau_+ \sigma_+ + \tau_+ \sigma_- + \tau_- \sigma_+) + \frac{10}{7} (1/2 + \tau_z)(\sigma_+ + \sigma_-) + \frac{18}{7} (1/2 - \tau_z)(\sigma_+ + \sigma_-) \right) \\
 &= 2\mu_B \sigma_x \left(1 + \frac{4}{7} (\sqrt{3}\tau_x - \tau_z) \right). \tag{A1}
 \end{aligned}$$

Another example is for Q_{xy} [see Eqs. (10)]:

$$Q_{xy} = Q_0 \left(i \frac{\sqrt{3}}{8} [\tau_-(1/2 + \sigma_z) + \tau_+(1/2 - \sigma_z)] - i \frac{\sqrt{3}}{8} [\tau_+(1/2 + \sigma_z) + \tau_-(1/2 - \sigma_z)] \right) = \frac{\sqrt{3}}{2} \sigma_z \tau_y = \mu_z. \tag{A2}$$

APPENDIX B

The original parameters $\mathcal{A}_{ij,mn}(\mathbf{r})$ give rise to $\mathcal{A}_{\alpha\beta}(\mathbf{r})$ and $\mathcal{B}_{ij}(\mathbf{r})$ whose angular dependence is derived below in accordance with Eqs. (11), (12), (15):

$$\mathcal{A}_{zz} = \mathcal{A}_{xx,xx} + \mathcal{A}_{yy,yy} + 4\mathcal{A}_{zz,zz} + 2\mathcal{A}_{xx,yy} - 4\mathcal{A}_{xx,zz} - 4\mathcal{A}_{yy,zz} = \frac{35}{24} (1 - 3n_z^2)^2 + \frac{5}{6} (1 - 3n_z^2) - \frac{7}{6},$$

$$\mathcal{A}_{xx} = 3\mathcal{A}_{xx,xx} + 3\mathcal{A}_{yy,yy} - 6\mathcal{A}_{xx,yy} = \frac{35}{8} (n_x^2 - n_y^2)^2 - \frac{5}{6} (1 - 3n_z^2) - \frac{7}{6},$$

$$\mathcal{A}_{xz} = \sqrt{3} (-\mathcal{A}_{xx,xx} + \mathcal{A}_{yy,yy} + 2\mathcal{A}_{xx,zz} - 2\mathcal{A}_{yy,zz}) = \sqrt{3} (n_x^2 - n_y^2) \left(-\frac{35}{24} (1 - 3n_z^2) + \frac{5}{6} \right).$$

$$\mathcal{B}_{xx} = 4\mathcal{A}_{yz,yz} = \frac{35}{6} n_y^2 n_z^2 + \frac{5}{6} n_x^2 - \frac{2}{3}, \quad \mathcal{B}_{yy} = 4\mathcal{A}_{zx,zx} = \frac{35}{6} n_z^2 n_x^2 + \frac{5}{6} n_y^2 - \frac{2}{3},$$

$$\mathcal{B}_{zz} = 4\mathcal{A}_{xy,xy} = \frac{35}{6} n_x^2 n_y^2 + \frac{5}{6} n_z^2 - \frac{2}{3}, \quad \mathcal{B}_{xy} = 4\mathcal{A}_{yz,xz} = \frac{5}{6} n_x n_y (7n_z^2 - 1),$$

$$\mathcal{B}_{yz} = 4\mathcal{A}_{zx,xy} = \frac{5}{6} n_y n_z (7n_x^2 - 1), \quad \mathcal{B}_{zx} = 4\mathcal{A}_{xy,yz} = \frac{5}{6} n_z n_x (7n_y^2 - 1).$$

To shorten the \mathcal{A} and \mathcal{B} expressions we skip their r dependence, i.e., factor r^{-5} .

Listed below are a few coupling constants of the effective σ - σ Hamiltonian (19):

$$\begin{aligned}\tilde{\mathcal{B}}_{xx}(\mathbf{a}_x) &= 0.0049, & \tilde{\mathcal{B}}_{yy}(\mathbf{a}_x) &= \tilde{\mathcal{B}}_{zz}(\mathbf{a}_x) = -0.0195, & \tilde{\mathcal{B}}_{yy}(\mathbf{a}_y) &= 0.0049, & \tilde{\mathcal{B}}_{xx}(\mathbf{a}_y) &= \tilde{\mathcal{B}}_{zz}(\mathbf{a}_y) = -0.0195, \\ \tilde{\mathcal{B}}_{zz}(\mathbf{a}_z) &= -0.0010, & \tilde{\mathcal{B}}_{xx}(\mathbf{a}_z) &= \tilde{\mathcal{B}}_{yy}(\mathbf{a}_z) = 0.0039, & \tilde{\mathcal{B}}_{zz}(\mathbf{a}_x \pm \mathbf{a}_y) &= -0.0011, & \tilde{\mathcal{B}}_{xy}(\mathbf{a}_x \pm \mathbf{a}_y) &= \pm 0.0006.\end{aligned}$$

APPENDIX C

Because of the rotational symmetry of the \mathbf{Q} -modulated state, we choose the quantization axis, \mathbf{n}_0 , as lying in the (τ_x, τ_z) plane. One of the two perpendicular directions, \mathbf{n}_1 , is taken also in the (τ_x, τ_z) plane. Let the third direction coincide with τ_y :

$$\mathbf{n}_0 = (\sin\phi, 0, \cos\phi), \quad \mathbf{n}_1 = (\cos\phi, 0, -\sin\phi), \quad \mathbf{n}_2 = (0, 1, 0).$$

In the spin-wave approximation

$$\boldsymbol{\tau} \cdot \mathbf{n}_0 = e^{i\mathbf{Q}\mathbf{r}} \left(\frac{1}{2} - b^\dagger b \right), \quad \boldsymbol{\tau} \cdot \mathbf{n}_1 = \frac{1}{2} e^{i\mathbf{Q}\mathbf{r}} (b + b^\dagger), \quad \boldsymbol{\tau} \cdot \mathbf{n}_2 = \frac{1}{2i} (b - b^\dagger).$$

Hence, to the same order we obtain

$$\tau_x = e^{i\mathbf{Q}\mathbf{r}} \left[\left(\frac{1}{2} - n \right) \sin\phi + \frac{1}{2} (b + b^\dagger) \cos\phi \right], \quad \tau_z = e^{i\mathbf{Q}\mathbf{r}} \left[\left(\frac{1}{2} - n \right) \cos\phi - \frac{1}{2} (b + b^\dagger) \sin\phi \right], \quad \tau_y = \frac{1}{2i} (b - b^\dagger). \quad (\text{C1})$$

Now operators (C1) can be used for extracting the ‘‘classical’’ and ‘‘spin-wave’’ parts of \mathcal{H}_{orb} :

$$\begin{aligned}& \sum_{\mathbf{r} \neq \mathbf{r}'} [\mathcal{A}_{zz}(\mathbf{r} - \mathbf{r}') \tau_z(\mathbf{r}) \tau_z(\mathbf{r}') + \mathcal{A}_{xx}(\mathbf{r} - \mathbf{r}') \tau_x(\mathbf{r}) \tau_x(\mathbf{r}') + \mathcal{A}_{xz}(\mathbf{r} - \mathbf{r}') (\tau_x(\mathbf{r}) \tau_z(\mathbf{r}') + \tau_z(\mathbf{r}) \tau_x(\mathbf{r}'))] \\ &= \sum_{\mathbf{q}} \left(\frac{1}{4} - b_{\mathbf{q}}^\dagger b_{\mathbf{q}} \right) \sum_{\mathbf{r}} e^{i\mathbf{Q}\mathbf{r}} [\mathcal{A}_{zz}(\mathbf{r}) \cos^2\phi + \mathcal{A}_{xx}(\mathbf{r}) \sin^2\phi + \mathcal{A}_{xz}(\mathbf{r}) \sin 2\phi] \\ &+ \frac{1}{4} \sum_{\mathbf{q}} \sum_{\mathbf{r}} e^{i\mathbf{Q}\mathbf{r}} e^{i\mathbf{q}\mathbf{r}'} [\mathcal{A}_{zz}(\mathbf{r}) \sin^2\phi + \mathcal{A}_{xx}(\mathbf{r}) \cos^2\phi - \mathcal{A}_{xz}(\mathbf{r}) \sin 2\phi] (b_{-\mathbf{q}} + b_{\mathbf{q}}^\dagger) (b_{\mathbf{q}} + b_{-\mathbf{q}}^\dagger).\end{aligned} \quad (\text{C2})$$

The ‘‘classical,’’ i.e., operator-independent, part of the right-hand side of Eq. (C2) is invariant under the rotation of \mathbf{n}_0 in the (τ_z, τ_x) plane (ϕ rotation). In fact, this part appears to be ϕ independent: $N\mathcal{A}_{\mathbf{Q}}/4$.

APPENDIX D:

Let us first divide both fields, $\boldsymbol{\sigma}$ and $\boldsymbol{\tau}$, into uniform and modulated parts:

$$\boldsymbol{\sigma}(\mathbf{r}) = \boldsymbol{\sigma}^{(0)} + \tilde{\boldsymbol{\sigma}}(\mathbf{r}), \quad \boldsymbol{\tau}(\mathbf{r}) = \boldsymbol{\tau}^{(0)} + \tilde{\boldsymbol{\tau}}(\mathbf{r}).$$

Then, the coefficients of the linear in $\tilde{\boldsymbol{\sigma}}$ and $\tilde{\boldsymbol{\tau}}$ terms in the exponential of Eq. (25) must be put zero, and we obtain

$$\begin{aligned}\tilde{\sigma}_z(\mathbf{r}): -2\lambda_\sigma \sigma_z^{(0)} + 2\mu_B H \left(1 + \frac{8}{7} \tau_z^{(0)} \right) &= 0; & \tilde{\sigma}_x(\mathbf{r}): \sigma_x^{(0)} &= 0; & \tilde{\sigma}_y(\mathbf{r}): \sigma_y^{(0)} &= 0; \\ \tilde{\tau}_z(\mathbf{r}): -2(\lambda_\tau + \mathcal{A}_0) \tau_z^{(0)} + \frac{16}{7} \mu_B H \sigma_z^{(0)} &= 0; & \tilde{\tau}_x(\mathbf{r}): \tau_x^{(0)} &= 0; & \tilde{\tau}_y(\mathbf{r}): \tau_y^{(0)} &= 0.\end{aligned}$$

This yields

$$\tau_z^{(0)} = \frac{7}{8} \frac{z}{\lambda_\tau + \mathcal{A}_0 - z}, \quad \sigma_z^{(0)} = \frac{\mu_B H}{\lambda_\sigma} \frac{\lambda_\tau + \mathcal{A}_0}{\lambda_\tau + \mathcal{A}_0 - z},$$

where $z = (8\mu_B H/7)^2 / \lambda_\sigma$.

Then, extracting the constants and the contribution of the uniform components of $\boldsymbol{\sigma}$ and $\boldsymbol{\tau}$ fields (\mathcal{Z}_0), we arrive at the Gaussian integration over $\tilde{\boldsymbol{\sigma}}$ and $\tilde{\boldsymbol{\tau}}$ in \mathcal{Z} :

$$\begin{aligned}\mathcal{Z} &= \mathcal{Z}_0 \mathcal{Z}_1; & \mathcal{Z}_1 &= \prod_{\mathbf{r}} \int_{-\infty}^{\infty} d\tilde{\boldsymbol{\sigma}}(\mathbf{r}) \int_{-\infty}^{\infty} d\tilde{\boldsymbol{\tau}}(\mathbf{r}) \\ &\times \exp\left\{ -\lambda_\sigma \tilde{\boldsymbol{\sigma}}^2(\mathbf{r}) + \frac{16}{7} \mu_B H \tilde{\sigma}_z(\mathbf{r}) \tilde{\tau}_z(\mathbf{r}) - \lambda_\tau \tilde{\boldsymbol{\tau}}^2(\mathbf{r}) - \sum_{\mathbf{r}'} \mathcal{A}_{\alpha\beta}(\mathbf{r} - \mathbf{r}') \tilde{\tau}_\alpha(\mathbf{r}) \tilde{\tau}_\beta(\mathbf{r}') \right\},\end{aligned} \quad (\text{D1})$$

where $\mathcal{Z}_0 = \exp(-N\mathcal{F}_0/T)$ and

$$-\mathcal{F}_0 = \frac{3}{4}\lambda_\sigma + \frac{1}{2}\lambda_\tau + \left(\frac{7}{8}\right)^2 \left(z + \frac{z^2}{\lambda_\tau + \mathcal{A}_0 - z} \right). \quad (\text{D2})$$

The $\tilde{\sigma}$ integration can be easily performed. It results in the contribution

$$-\mathcal{F}_1^{(\sigma)} = \frac{3}{2} T \ln \frac{\pi T}{\lambda_\sigma}, \quad (\text{D3})$$

and transforms $\mathcal{A}_{zz}(\mathbf{r}-\mathbf{r}') \rightarrow \mathcal{A}_{zz}(\mathbf{r}-\mathbf{r}') - \delta_{\mathbf{r},\mathbf{r}'} z$.

Thus, we can rewrite \mathcal{Z}_1 as $\exp[-N(\mathcal{F}_1^{(\sigma)} + \mathcal{F}_1^{(\tau)})/T]$, and

$$\exp - \frac{N\mathcal{F}_1^{(\tau)}}{T} = \prod_{\mathbf{r}} \int_{-\infty}^{\infty} d\tilde{\tau}(\mathbf{r}) \exp - \beta \sum_{\mathbf{r}'} \tilde{\mathcal{A}}_{\alpha\beta}(\mathbf{r}-\mathbf{r}') \tilde{\tau}_\alpha(\mathbf{r}) \tilde{\tau}_\beta(\mathbf{r}'), \quad (\text{D4})$$

where

$$\tilde{\mathcal{A}}_{zz}(\mathbf{r}) = \delta_{\mathbf{r},0}(\lambda_\tau - z) + \mathcal{A}_{zz}(\mathbf{r}), \quad \tilde{\mathcal{A}}_{xx}(\mathbf{r}) = \delta_{\mathbf{r},0}\lambda_\tau + \mathcal{A}_{xx}(\mathbf{r}), \quad \tilde{\mathcal{A}}_{xz}(\mathbf{r}) = \mathcal{A}_{xz}(\mathbf{r}).$$

The functional integration in Eq. (D4) can be straightforwardly performed:

$$-\mathcal{F}_1^{(\tau)} = \frac{T}{2} \frac{1}{N} \sum_{\mathbf{k}} \ln \frac{(\pi T)^2}{\tilde{\mathcal{A}}^{zz}[\mathbf{k}] \tilde{\mathcal{A}}^{xx}[\mathbf{k}] - (\tilde{\mathcal{A}}^{xz}[\mathbf{k}])^2}. \quad (\text{D5})$$

*On leave from Landau Institute for Theoretical Physics, Chernogolovka, Moscow District 142432, Russia.

¹K. Winzer and W. Flesch, J. Phys. (Paris) Colloq. **39**, C6-832 (1978).

²A. Takase, K. Kojima, T. Komatsubara, and T. Kasuya, Solid State Commun. **36**, 461 (1980).

³N. Sato, S. Kunii, I. Oguro, T. Komatsubara, and T. Kasuya, J. Phys. Soc. Jpn. **53**, 3967 (1984).

⁴E. Zirngiebl, B. Hillebrands, S. Blumenröder, G. Güntherodt, M. Loewenhaupt, J. Carpenter, K. Winzer, and Z. Fisk, Phys. Rev. B **30**, 4052 (1984).

⁵P. Burlet, J.X. Boucherle, J. Rossat-Mignod, J.W. Cable, W.C. Koehler, S. Kunii, and T. Kasuya, J. Phys. (Paris) Colloq. **43**, C7-273 (1982).

⁶F.J. Ohkawa, J. Phys. Soc. Jpn. **52**, 3897 (1983).

⁷K.N. Lee and B. Bell, Phys. Rev. B **6**, 1032 (1972).

⁸T. Fujita, M. Suzuki, T. Komatsubara, S. Kunii, T. Kasuya, and T. Ohtsuka, Solid State Commun. **35**, 569 (1980).

⁹Y. Peysson, C. Ayache, J. Rossat-Mignod, S. Kunii, and T. Kasuya, J. Phys. (Paris) **47**, 113 (1986).

¹⁰M. Kawakami, K. Mizuno, S. Kunii, T. Kasuya, H. Enokiya, and K. Kume, J. Magn. Magn. Mater. **30**, 201 (1982).

¹¹M. Takigawa, H. Yasuoka, T. Tanaka, and Y. Ishizawa, J. Phys. Soc. Jpn. **52**, 728 (1983).

¹²S. Horn, F. Steglich, M. Loewenhaupt, H. Scheuer, W. Flesch, and K. Winzer, Z. Phys. B **42**, 125 (1981).

¹³J.M. Effantin, J. Rossat-Mignod, P. Burlet, H. Bartholin, S. Kunii, and T. Kasuya, J. Magn. Magn. Mater. **47-48**, 145 (1985).

¹⁴G. Uimin, Y. Kuramoto, and N. Fukushima, Solid State Commun. **97**, 595 (1996).

¹⁵W.A.C. Erkelens, L.P. Regnault, P. Burlet, J. Rossat-Mignod, S. Kunii, and T. Kasuya, J. Magn. Magn. Mater. **63-64**, 61 (1987).

¹⁶A. Lacerda and M. Torikachvili (unpublished).

¹⁷R. Feyherherm, A. Amato, F.N. Gyax, A. Schenck, Y. Ōnuki, and N. Sato, Physica B **194-196**, 357 (1994); J. Magn. Magn. Mater. **140-144**, 1175 (1995).

¹⁸B. Bleaney, Proc. Phys. Soc. (London) **77**, 113 (1961).

¹⁹R.J. Birgeneau, M.T. Hutchings, J.M. Baker, and J.D. Riley, J. Appl. Phys. **40**, 1070 (1969).

²⁰P.M. Levy, P. Morin, and D. Schmitt, Phys. Rev. Lett. **42**, 1417 (1979).

²¹According to Ref. 20 the value of the direct quadrupolar interaction in some intermetallic rare-earth compounds is of order 10^{-3} K. That estimate should be consistent with a large screening effect on a quadrupolar moment by outer electrons, which is unlikely the case of CeB₆.

²²J. Hubbard, J. Phys. C **4**, 53 (1971).

²³K. Sugiyama, F. Iga, M. Kasaya, T. Kasuya, and M. Date, J. Phys. Soc. Jpn. **57**, 3946 (1988).

²⁴T. Matsumura *et al.* (unpublished).

²⁵For a detailed description of orientations and periodicities of such domains we may recommend the following theses: J.M. Effantin, Ph.D. thesis, Université de Grenoble, 1985; W.A.C. Erkelens, Ph.D. thesis, University of Leiden, 1987; A. Bouvet, Ph.D. thesis, Université J. Fourier, Grenoble, 1993.

²⁶P. Morin, and D. Schmitt, Phys. Lett. **73A**, 67 (1979).

²⁷G. Uimin, Phys. Lett. A **215**, 97 (1996).